3

Correction of NDVI calculated from ASTER L1B and ASTER (AST07) data based on ground measurement*

Hoshino Buho,
Masami Kaneko,
Kenta Ogawa
Rakuno Gakuen University, Japan

Abstract
atmospheric correction of the satellite data, for example correction of visible and near-infrared spectral bands, requires removing the adjacency effect that is due to the reflection from contiguous pixels. To evaluate the accuracy of the ATCOR software atmospheric correction method of Terra/ASTER data (Jun 30, 2002) we compared the NDVI parameters taken from different sources, such as ground measurement using ground radiometric measurement data (ASD's FieldSpec® Pro), atmospheric corrected ASTER L1B data and ASTER surface reflectance product (AST07) data. The study area named Sarobetsu Marsh is located in the coastal area of Hokkaido Island, Japan. It has been found that 5% of the scattering radiation is contained within the ASTER Green band, 47% of radiation was absorbed in the ASTER NIR band and 17% of radiation was absorbed in the ASTER SWIR6 band, respectively. There was no significant difference between ASD's measurement values and the ATCOR software output values in the ASTER reflection band and absorption bands of chlorophyll (i.e. NIR-band and Red-band). However, differences were seen in the ASTER scattering bands (i.e. visible Green band) and soil reflection bands (i.e. ASTER SWIR bands). Comparison of the original ASD's ground measurement data with the AST07 (©NASA/EOSDIS ASTER surface reflectance product data (L2B) values has revealed very low reflectance of a NIR band.

Keywords: NDVI, ASTER L1B & AST07, ASD's FieldSpec®, surface reflectance, ground measurment.

1. Introduction

The electromagnetic (EM) energy travels through the atmosphere from the sun to target remote sensing sensors. Radiation from the Earth's surface undergoes significant interaction with the atmosphere before it reaches the satellite sensors. Regardless of the type of analysis that is performed on the remotely sensed data, it is important to understand the effect the

atmosphere has made to the radiance responses [1]. In order to acquire an exact radiation of target, we must correct the atmosphere effect of satellite imagery. Correction of image data for the effects of atmospheric propagation can be carried out essentially in three ways [2]. It is respectively, based on atmospheric scattering and absorption characteristics of the physical model; based on pre-calibration, on-board calibration against targets of known reflectance method and based on dark-pixel subtraction method. The physically based methods of attempt to model (for example, Look-up table (LUT) approach and top-of atmosphere (TOA) radiance) is the most rigorous approach, and also the most difficult to apply [3] [4]. The atmospheric scattering and absorption characteristics area calculated by a computer model such as the LOWTRAN-7 [4], MODTRAN [5] [6] and 6S [7] require to input meteorological, seasonal and geographical data. In practice, these variables may not be available with sufficient spatial or temporal resolution, and, in particular, estimation of the contribution of atmospheric aerosols is difficult [3] [8]. In the calibration based atmospheric correction of VNIR (visible and near infrared), SWIR (short-wave infrared) imagery method, these targets can be artificially constructed or naturally occurring, but they need to satisfy a number of criteria[3]: (1) their reflectances must be known sufficiently accurate, in the same spectral bands as are used by the imager; (2) the range of reflectances represented by the calibrators must span the range of interest in the sensor; (3) each calibrator should cover an area of at least several resolution elements; (4) the calibrators should be well distributed over the entire scene, so that possible variation of atmospheric conditions from place to place can be assessed and if necessary, allowed for [3]. Dark pixel subtraction is a technique that determines the pixel in the image with the lowest brightness value. This method is quite crude: it is that the minimum reflectance in each band is zero, that the atmospheric correction can be modeled adequately as an additive effect, and that the correction does not vary from place to place within the scene. To some extent, visual inspection of an image can determine whether these assumptions are likely to be valid. Zero-reflectance resolution element can be provided by shadows, and in the near-infrared region, by water bodies [3] [5] [7]

In this study, we evaluated the accuracy of the atmosphere correction with ATCOR atmospheric correction algorithm based on ground radiometric measurement data, and compared also with the radiative transfer code (RTC) based atmospheric corrected ASTER L2B standard products surface reflectance (AST07) data simultaneously.

1.1 ATCOR algrithm atmospheric correction method

Rayleigh scattering of sunlight in clear atmosphere is the main reason why the sky is blue. Since blue light is at the short wavelength end of the visible spectrum, it is more strongly scattered in the atmosphere than long wavelength red light. The result is that the human eye perceives blue when looking toward parts of the sky other than the sun [9]. So the atmospheric effects are much larger in these blue band images. As is known to all, healthy live green plants absorb solar radiation in the photosynthesis active radiation spectral (i.e. visible Red) region, which they use as a source of energy in the process of photosynthesis. Leaf cells have also evolved to scatter solar radiation in the near-infrared (NIR) spectral region, because the energy level per photon in that domain is not sufficient to be useful to synthesize organic molecules: a strong absorption here would only result in over-heating the plant and possibly damaging the tissues. Hence, live green plants appear relatively dark in

the PAR (Photosynthesis Active Radiation) and relatively bright in the NIR [10]. By contrast, clouds and snow tend to be rather bright in the red (as well as other visible wavelengths) and quite dark in the NIR.
The ATCOR program can correct the path radiance, adjacency radiation and terrain radiation reflected to the pixel in order to calculate the reflected radiation from the viewed pixel. ATCOR2 algorithm atmospheric correction algorithm is for a flat terrain working with an atmospheric database, and ATCOR3 algorithm can correct terrain radiation reflected to the pixel (from opposite hills, according to the terrain view factor). The database that contains the atmospheric correction functions is stored in LUT. ATCOR does the atmospheric correction by inverting the results obtained from MODTRAN, are stored in a Look up Table. If anything, the ATCOR algorithm method is kind of applied to the above-mentioned method of the physically based methods attempt to model [11] [12] [13].

1.2 The ASTER surface reflectance product (AST07) algorithm

The validated version of the VNIR/SWIR surface leaving radiance and reflectance products (product name: ((c) NASA/EOSDIS) AST07) provide an estimate of the total radiance leaving the surface including both the reflected solar and sky components for ASTER bands 1-9. The atmospheric correction for the VNIR and SWIR is based upon LUT approach using results from a Gauss-Seidel iteration radiative transfer code [14]. The method has its basis in the reflectance-based, vicarious-calibration approach of the Remote Sensing Group at the University of Arizona [15]. We are applying the knowledge learned from our calibration methods to the atmospheric correction of the VNIR and SWIR bands for ASTER. Specifically, the RTC we have used for the past 10 years is used as a basis for LUT approach to atmospheric correction. The method currently assumes atmospheric scattering optical depths and aerosol parameters are known from outside sources. Using these parameters, a set of piecewise-linear fits are determined from the LUT that relates the measured satellite radiances to surface radiance and surface reflectance [16] [17].

2. The dara analyzed in this study

2.1 Resampling the original ASTER data

Wetland monitoring, particularly wetland vegetation classification, is crucial for preserving valuable wetland ecosystems. The development of remote sensing techniques for wetland monitoring is urgent. To improve the accuracy of vegetation classification, we have investigated wetland vegetation classification with multi-temporal ASTER images. However, for many quantitative applications of ASTER VIR imagery (e. g. calculated the ASTER NDVI), it is desirable to correct the data for the effects of atmospheric propagation. If the data is accurately calibrated, the variable that is measured is the radiance ($W.sr^{-1}.m^{-2}$) reaching the sensor. But the variable that is wanted is the reflectance (%) of the surface. In this study we approach to make an atmospheric correction of ASTER VIR imagery based on calibration against targets of known reflectance. The ground targets object is wetland area, and the land cover types including water surface, bare soil and green vegetation.
The Advanced Spaceborne Thermal Emission and Reflection Radiometer (ASTER) onboard NASA's satellite Terra is a high resolution multispectral radiometer with 14 bands that

covers the visible and near-infrared (VNIR), short wave infrared (SWIR) and thermal infrared (TIR), and is effective in studying the Earth's surface land cover, vegetation and mineral resources, etc. We used data from Terra/ASTER original Level 1B VNIR / SWIR/TIR Data (Time of day (UTC): 1:30, June 30, 2003, Path-108/Row-835, and 1:30, July 12, 2004, Path-109/Row-837, the subset coordinate of the UL Geo N45° 08′, E141° 36′) supplied by the Earth Remote Sensing Data Analysis Center, Tokyo, Japan (©ERSDAC). In the ATCOR software, if a 14-bands ASTER image is loaded the default Layer-Band assignment will be set that input layer 13 (thermal band 13) is set to layer 10 and the output image will be restricted to 10 bands. The reason for this is that from the 5 ASTER thermal bands only band 13 is used in ATCOR. In order to carry out calculation between bands, we re-sampled (layer stacking) this 3 layers with different spatial resolution ASTER VNIR (15 m), SWIR (30 m) and TIR (90 m) data to one layer that has the same spatial resolution (15 m) dataset, and used this dataset input to ATCOR software.

2.2 ATCOR input parameters

With the ASTER data (Path-108/Row-835), ATCOR input parameters include: Solar zenith (degrees): **24.8**; Solar azimuth (degrees): **147.7**; Scene Visibility (km) = **30**m; Model for solar region; fall/spring/rural; various aerosol types: **rural**; Model for thermal region: **fall**. Input satellite data: subset ASTER VNIR-SWIR-TIR, **10-bands** one layer data. In the calibration of ASTER data the Level 1B data is in terms of scaled radiance. The unit conversion coefficients (defined as radiance per 1 DN) are shown in Table 1. Radiance (spectral radiance) is expressed in units of **W/(m2*sr*um)**. The true radiance at sensor can be obtained from the DN values as follows:

$$L = c_0 + c_1 \times DN \tag{1}$$

Where, L is radiance, c_0 (offset) and c_1 (gain) is conversion coefficient; DN is digital number.

Band No.	c_0	c_1
1	-0.1	0.0676
2	-0.1	0.0708
3	-0.1	0.0862
4	-0.1	0.02174
5	-0.1	0.00696
6	-0.1	0.00625
7	-0.1	0.00597
8	-0.1	0.00417
9	-0.1	0.00318

Table 1. The calibration of ASTER original L1B data (Unit: mW/cm2 sr micron)

3. The study area

The study area Sarobetsu Marsh, is the largest registered wetland of 7000 ha located in coastal area of northwestern Hokkaido, Japan (Figure 1) and nominated by the Ramsar Convention on Wetlands in 2005. Test areas are mostly swamp with *Sphagnum* sp., *Moliniopsis japonica* while the western coastal zone area is dominated by isolated small hills covered with broad-leaf trees. The terrain of the study area is very flat with the elevation distributed between 5 m to 15 m. The area was selected because of its natural environment and perseverance by national and municipal governments. On the other hand recently the expansion of a non-moor plant (bamboo grass) has been detected in a swamp. So far, for the monitoring, the classification of the wetland territory into a high moor, low moor and non moor types, to clarify the invasion front of bamboo grass is very important.

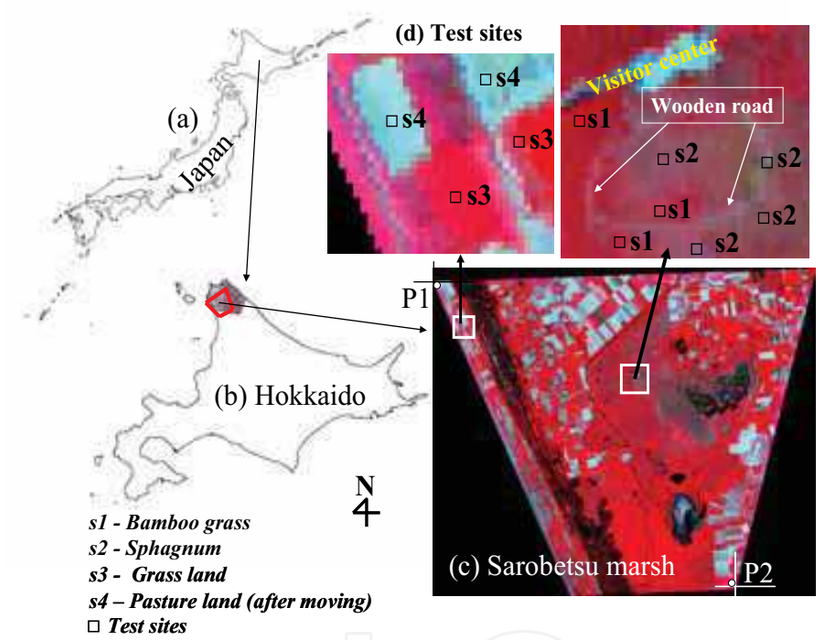

Fig. 1. Location of study area and test sites

4. Result

The atmospheric correction processing evaluated within this chapter is to a major part based on the technology of the ATCOR-3 atmospheric correction procedure [11][12]. In this algorithm, the total signal at the sensor consists of four components: (1)-path radiance; (2)-reflected radiation from the viewed pixel; (3)-scattered radiation from the neighborhood; and (4)-terrain radiation reflected to the pixel. Figure 2. shows the result of ATCOR atmospheric corrected ASTER data in the test area. The satellite scene has to be ortho-rectified to a DEM (digital elevation model) before the ATCOR3 processing starts. The influence of the neighborhood is neglected. A start value for the ground reflectance of the surrounding topography is employed whilst the path radiance component is subtracted

from the signal. Shadow cast from surrounding topography is included. However, as our study area is very flat, the topography effect is rare. Haze removal is the important steps prior to the application of imagery. This result shows the ATCOR algorithm is a more effective haze removal and atmospheric correction modeling which combined several improved methods (see Fig. 2(c)).

The global flux on the ground depends on the large-scale (1 km) average reflectance. The global flux in the atmospheric LUT's is calculated for a fixed reflectance=0.15 . This iteration performs the update for the spatially varying average reflectance map of the current scene, if the adjacency range R > 0 [10]. The empirical BRDF correction is areas of low illumination (see Fig. 2(b)).

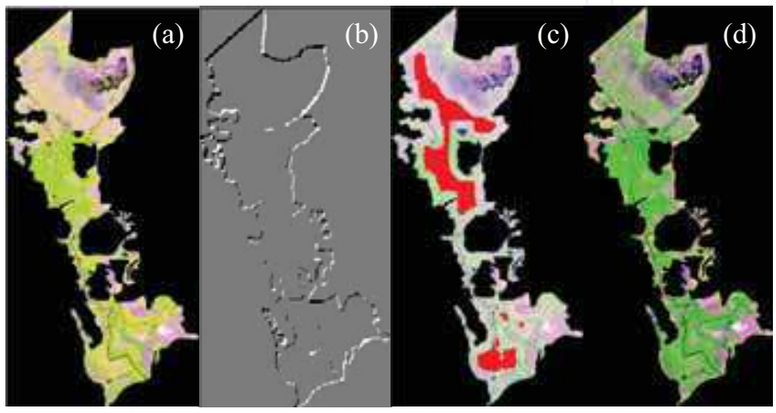

Fig.2. Result of the ATCOR3 correction. (a) original ASTER/L1B data; (b) the illumination azimuth angle ; (c) hazeoverlay; (d) atmospheric corrected ASTER data.

Comparison of the ASTER data before and after ATCOR software atmospheric correction has revealed following results:

(a) The mean values of ASTER band 1 and band 2 decrease after atmospheric correction (Table 2). This means that the visible green and red band has included not only the radiance from a target, but also radiance other than an atmospheric scattering is also included.

(b) Comparison of mean values of NIR and SWIR bands before/after atmospheric correction shows that the radiance values became larger after atmospheric correction. It means that the radiation from the target is absorbed by atmosphere before it reaches the satellite sensor. Atmospheric scattering primarily affects the direction of visible Green and Red band, and atmospheric absorption primarily affects the direction of NIR and SWIR bands.

The most significant interaction that undergoes by the thermal infrared radiation when it passes through the atmosphere is its absorption, primarily due to ozone and water vapor particles in the atmosphere. At the visible shorter wavelengths (i.e. Green or Red band), attenuation occurs by scattering due to clouds and other atmospheric constituents, as well as reflection. The type of scattering in which the energy undergoes is depends upon the size of the particle. Rayleigh scattering occurs when radiation interacts with air molecules smaller than the radiation's wavelength, such as oxygen and nitrogen. The degree of scattering is inversely proportional to the fourth power of the wavelength. When particles are

comparable in size to the radiation wavelength, such as aerosols, it results in Mie scattering type [18]. The effect of scattering on the visible wavelengths is significant and must be compensated for when developing empirical relationships through time [19] [20]. Atmospheric scattering primarily affects the direction of short wave radiation. There are four types of atmospheric scattering: Rayleigh, Mie, Raman and non selective. The most significant of these types of scattering is Rayleigh scatter, which effects the short visible wavelengths and results in haze. For ASTER data the scattering is four times as great in Green band of the electromagnetic spectrum as in the NIR band [21],[22].

DN of original ASTER L1B data (before correction)				
Band No.	Min	Max	**Mean**	St dev
1 (Green)	0	255	**50.93**	34.97
2 (red)	0	210	**30.83**	23.15
3 (NIR)	0	179	**69.82**	49.02
4 (SWIR)	0	111	**45.21**	32.59
5 (SWIR)	0	105	**27.82**	20.52
6 (SWIR)	0	144	**29.90**	22.66
7 (SWIR)	0	155	**27.49**	20.41
8 (SWIR)	0	191	**23.83**	18.10
9 (SWIR)	0	133	**21.01**	15.20
DN after ATCOR correction of ASTER data				
1 (Green)	0	229	**26.47**	20.16
2 (Red)	0	255	**30.04**	26.17
3 (NIR)	0	255	**93.53**	66.98
4 (SWIR)	0	224	**90.89**	65.64
5 (SWIR)	0	175	**46.17**	34.13
6 (SWIR)	0	251	**51.75**	39.30
7 (SWIR)	0	241	**42.42**	31.55
8 (SWIR)	0	255	**35.86**	27.33
9 (SWIR)	0	157	**24.34**	17.69

Table 2. Comparison of DN before and after ATCOR atmospheric correction of ASTER data ((Path-108/Row-835, UTC: 1:30, June 30, 2002)

Figure 3(1) and 3(2) shows that the ASD's measurement values and the ATCOR output values have no big difference in the ASTER reflection bands and absorption bands of chlorophyll (i.e. NIR-band and Red-band); the difference has come out in scattering band (i.e. ASTER Green band) and soil reflection bands (i.e. ASTER SWIR bands). However, in the ©EOSDIS AST07 (ASTER surface reflectance products), the values are considerably different in ASTER NIR band. The problem is in low values of NIR after atmospheric correction. In this research, the results of ATCOR software correction were better than those of AST07 products. Figure 3(1) and 3(2) shows the comparison of ATCOR software atmospheric correction result and ASTER surface reflectance products (AST07) data, in non moor and high moor plant samples. In a swamp (high moor plant), the background soil and the open water area will be incorrectly recognized as moving haze of ATCOR software method. After ATCOR correction the ASTER SWIR bands values are becomes larger following the changes

of vegetation due to dryness.

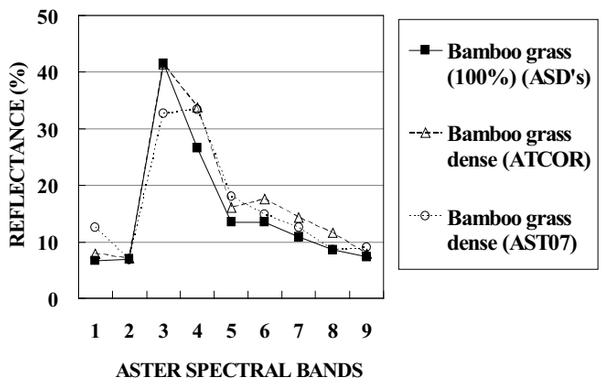

Fig. 3 (1) Comparison of the spectral reflectance of non-moor plant Bamboo grass calculated form ASD's measurement method, ATCOR method and EOSDIS AST07 method.

ATCOR have rectified more correctly scattering with short wavelength visible ((i.e. Band 1 (Green)) and absorption with NIR band (Band 3). The Fig. 4(1) and 4(2) clearly shows that 5% of scattering radiation is contained with the green band and 47% of radiation was absorbed in the NIR band and 17% of radiation was absorbed in the SWIR6 band.

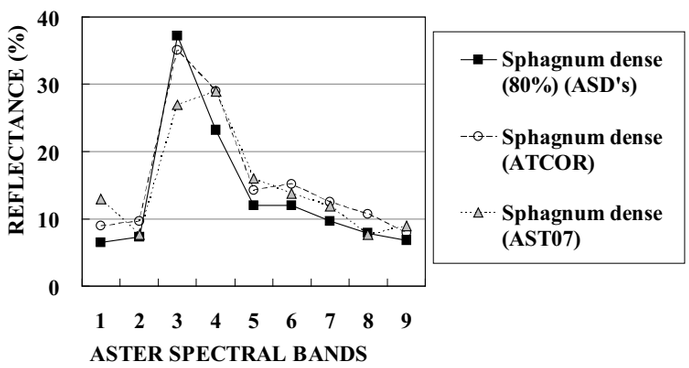

Fig. 3 (2) Comparison of the spectral reflectance of high moor plant *Sphagnum* marsh calculated form ASD's measurement method, ATCOR method and EOSDIS AST07 method.

The input (x: DN of original ASTER L1B data) and output (y: DN of after ATCOR software atmospheric corrected ASTER L1B data) expression of the ASTER data using ATCOR are as follows:

$$\text{Green band (band 1):} \quad y = 0.95x - 28.56 \tag{2}$$

$$\text{NIR band (band 3):} \quad y = 1.473x - 21.12 \tag{3}$$

$$\text{SWIR band (band 6):} \quad y = 1.171x - 1.23 \tag{4}$$

Comparing NDVI from ground ASD's measurement, corrected ASTER data and not corrected original ASTER L1B data (see Figure 4(3)), we found that values from the ground

NDVI and atmospheric corrected NDVI did not greatly differed. However, the value of NDVI of ASTER L1B is smaller than the value of grand NDVI. The formula of the correlation of a NDVI-Corrected value and an original ASTER L1B NDVI value is as follows:

$$NDVI_{corrected} = 1.27 \times NDVI_{L1B} + 0.04 \tag{5}$$

This formula showed that the NDVI value after atmospheric correction became larger than that before atmospheric correction.

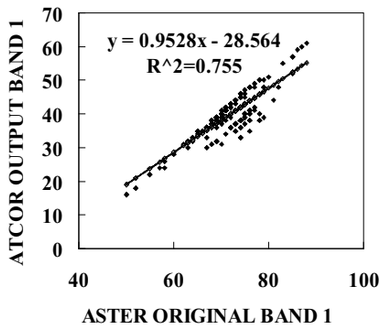

Fig. 4(1) The correlation coefficient of the ASTER original band 1 (Green) and ATCOR output band 1 (Green).

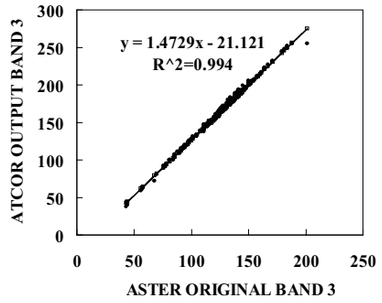

Fig. 4(2) The correlation coefficient of the ASTER original band 3 (NIR) and ATCOR output band 3 (NIR)

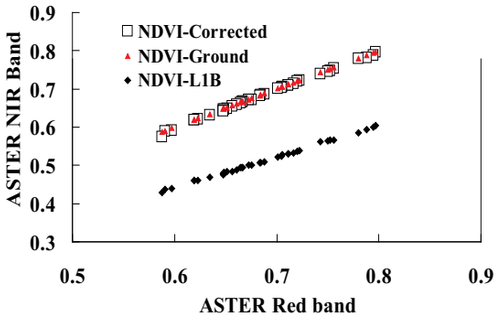

Fig. 4(3) Comparison of NDVI of ground measurement, atmospheric corrected ASTER L1B data and not atmospheric corrected original ASTER L1B data

5. Conclusion

Many techniques have been developed to determine the contribution of atmospheric scattering has on the radiation detected by the satellite sensor. The radiance received from a target against a background surface by the satellite sensor comes from a combination of three sources; first, the intrinsic radiance reflected by the target and then directly transmitted by the atmosphere; secondly, the radiant energy scattered diffusely by the atmosphere which then further interacts with the target background; thirdly, the radiant energy scattered diffusely by the atmosphere. The radiant energy reflected by the target carries the direct energy from the target. The other two sources produce a combined effect.
Atmospheric measurements and modeling involve the theoretical determination of the path radiance contribution of the atmosphere for the particular time of the overpass. To calculate the contribution of the scattering on the reflected radiance requires that many atmospheric variables at the time of the satellite overpass be recorded and input into theoretically derived equations to determine the effect of the atmosphere on each spectral band.
Correction of image data for the effects of atmospheric propagation can be carried out essentially in three ways. It is respectively, 1) based on atmospheric scattering and absorption characteristics of model; 2) based on pre-calibration, on-board calibration against targets of known reflectance method and 3) based on dark-pixel subtraction method. The physic based methods are the most rigorous approach, and also the most difficult to apply. The atmospheric scattering and absorption characteristics area calculated by a computer model requires meteorological, seasonal and geographical variables. In practice, these variables may not all be available with sufficient spatial or temporal resolution, and in particular, estimation of the contribution of atmospheric aerosols is difficult. Other methods mentioned also have a number of requirements that are not easy to satisfy.
In this study, the accuracy of the atmospheric correction with ATCOR software algorithm was based on the usage of ground radiometric measurement data, which were compared also with the radiative transfer code (RTC) that is based on atmospheric corrected ASTER L2B standard products surface reflectance (AST07) data simultaneously.
The NDVI data calculated from ground measurement, atmospheric corrected ASTER L1B data and ASTER surface reflectance product (AST07) data was used to evaluate the accuracy of the ATCOR software atmospheric correction of Terra/ASTER data (Jun 30, 2002). Ground measurements were done using ground radiometric measurement data (ASD's FieldSpec® Pro) at the study area named Sarobetsu Marsh located in coastal area of Hokkaido, Japan.
The study showed that the background soil and leaf area affected the accuracy of ATCOR. It has been found that 5% of scattering radiation is contained with the ASTER Green band and 47% of radiation was absorbed in the ASTER NIR band and 17% of radiation was absorbed in the ASTER SWIR6 band. The ground measurement values and the ATCOR software output values were of no big difference in the ASTER reflection band and absorption bands of chlorophyll (i.e. NIR-band and Red-band). However, the difference was seen in the ASTER scattering bands (i.e. visible Green band) and soil reflection bands (i.e. ASTER SWIR bands). Compared with the data of ASD's measurement, the AST07 (©NASA/EOSDIS ASTER surface reflectance product data (L2B)) values are too low in a NIR band.
For the ASTER original L1B data (Jun 30, 2001), the statistics mean value of Green band and NIR band is 50.9 and 69.8 after atmospheric correction, the statistics mean value of Green band and NIR band is 26.5 and 90.9. (For the ASTER/July 12, 2004 case, the values was 53.8

and 83.5 to 27.5 and 131.4 respectively). The value of NDVI after atmospheric correction is larger than atmospheric correction before, and this rate of change is (NDVI-Corrected) = 1.27 (NDVI-L1B) + 0.04.
Comparison of accuracy of the ATCOR software atmosphere correction of non-moor plant and high moor plant area ASTER imagery showed that the background soil and leaf area affected the accuracy of ATCOR. In the case of a moor plant, the error in ASTER Green band is large.

6. Acknowledgment

This work was supported by Grant-in-Aid for Scientific Research (A) 21370005 and the Global Environmental Research Fund (F-092) by the Ministry of the Environment, Japan.

7. References

[1] Schott J.R. and Henderson-Sellers, A., "Radiation, the Atmosphere and Satellite Sensors, Contribution in Satellite Sensing of a Cloudy Atmosphere: Observing the Third Planet (Ed: Henderson-Sellers), " 1984, pp45-89.
[2] Campbell, J. B., "Introdution to Remote Sensing: Second Edition," The Guilford Press, New York. 1996, pp. 444-476.
[3] W.G.Rees, " Physical Principles of Remote Sensing, Second Edition, " Cambridge University Press. 2001, pp. 76-85.
[4] Kneizys, F.X., "Atmospheric Transmittance Radiance: computer code " LOWTRANG AFGL-TR-83-0187 (1983).
[5] Berk, A., L. S. Bernstein, and D. C. Robertson, "MODTRAN. A Moderate Resolution Model for LOWTRAN 7,". GL-TR-89-0122, Phillips Laboratory, Geophysics Directorate, Hanscom Air Force Base, Massachusetts, 1989.
[6] Berk, A., L.S. Bernstein, G.P. Anderson, P.K. Acharya, D.C. Robertson, J.H., "Chetwynd and S.M. Adler-Golden, MODTRAN Cloud and Multiple Scattering Upgrades with Application to AVIRIS, ," Remote Sens. Environ, 1998, pp.65:367-375.
[7] E. Vermote, D. Tanr, J. Deuz, M. Herman, and J. Morcette, "Second simulation of the satellite signal in the solar spectrum 6S: An overview, " IEEE Trans. Geosci. Remote Sensing, vol. 35, no. 3, 1997, pp. 675—686.
[8] Fraser, R. S, R. A. Ferrare, Y. J. Kaufman, B. L. Markham, S. Mattoo, "Algorithm for atmospheric correction of aircraft and satellite imagery, " Int'l. J. Rem. Sens., 1992, pp.13:541-557.
[9] Nave, Carl Rod, 2005. Hyperphysics-Quantum Physics, Department of Physics and Astronomy, Georgia State University, CD.
[10] Gates, David M. (1980) Biophysical Ecology, Springer-Verlag, New York, pp. 611.
[11] R. Richter, "A fast atmospheric correction algorithm applied to Landsat TM, " Int. J. Remote Sensing 1990, pp.11:159-166.
[12] R. Richter, "Correction of atmospheric and topographic effects for high spatial resolution satellite imagery", Int. J. Remote Sensing 18:1099-1111 (1997).
[13] Richter, R. and Schläpfer, D., "Geo-atmospheric processing of airborne imaging spectrometry data. Part 2:Atmospheric/Topographic Correction". International Journal of Remote Sensing, 23(13): 2631-2649 (2002).

[14] Herman, B. M., & Browning, S. R., "A numerical solution to theequation of radiative transfer, " Journal of the Atmospheric Sciences, 22, 1965, pp.559-566.

[15] Slater, P. N., Biggar, S. F., Holm, R. G., Jackson, R. D., Mao, Y., Moran, M. M., Palmer, J. M., & Yuan, B., "Reflectance- and radiance-based methods for the in-flight absolute calibration of multispectral sensors, " Remote Sensing of Environment, 1987, pp.22, 11 – 37.

[16] .Aosier, B. Kaneko, M. Takada, M., Comparison of NDVI of ground measurement, atmospheric corrected ASTER L1B data and ASTER surface reflectance product (AST07) data, Geoscience and Remote Sensing Symposium, 2007 IEEE International; Barcelona,Spain, Publication Date: 23-28 July 2007, pp. 1806-1811.

[17] Buhe Aosier, K. Tsuchiya, M. kaneko, S. J. Saiha, "Comparison of Image Data Acquired with AVHRR, MODIS, ETM+, and ASTER Over Hokkaido Japan," *Advances in Space Research*, Vol. 32, No. 11, 2003, pp.2211-2216.

[18] Drury, S.A., "Image Interpretation in Geology. Allen and Unwin (Publishers) Ltd, London. Forster, B.C. (1980). Urban residential ground cover using Landsat digital data. Photogram, " Eng. Remote. Sen. 46, 547, 1987, pp.58.

[19] Coops, N.C., Culvenor, "Utilizing local variance of simulated high-spatial resolution imagery to predict spatial pattern of forest stands, " Remote Sensing of Environment. 71(3): 2000, pp.248-260.

[20] Jensen, J.R., 1986. 'Introductory Digital Image Processing : A Remote Sensing Perspective', New Jersey : Prentice-Hall.

[21] Crippen, R.E., "The Regression Intersection Method of Adjusting Image Data for Band Ratioing, " *International Journal of Remote Sensing.* Vol. 8. No. 2. 1987, pp. 137 155.

[22] Chavez, P. S., Jr., "An improved dark-object subtraction technique for atmospheric scattering correction of multispectral data ," *Remote Sens. Environ.*, 24, 1988, pp. 459-479.

[23] Herman, B. M., & Browning, S. R., "A numerical solution to theequation of radiative transfer, " Journal of the Atmospheric Sciences, 22, 1965, pp.559-566.

[24] Slater, P. N., Biggar, S. F., Holm, R. G., Jackson, R. D., Mao, Y., Moran, M. M., Palmer, J. M., & Yuan, B., "Reflectance- and radiance-based methods for the in-flight absolute calibration of multispectral sensors, " Remote Sensing of Environment, 1987, pp.22, 11 – 37.

* corresponding author Hoshino Buho: e-mail: aosier@rakuno.ac.jp

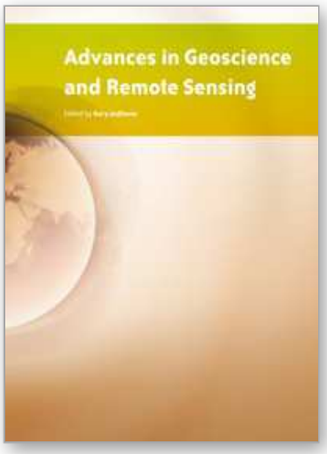

Advances in Geoscience and Remote Sensing

Edited by Gary Jedlovec

ISBN 978-953-307-005-6

Hard cover, 742 pages

Publisher InTech

Published online 01, October, 2009

Published in print edition October, 2009

Remote sensing is the acquisition of information of an object or phenomenon, by the use of either recording or real-time sensing device(s), that is not in physical or intimate contact with the object (such as by way of aircraft, spacecraft, satellite, buoy, or ship). In practice, remote sensing is the stand-off collection through the use of a variety of devices for gathering information on a given object or area. Human existence is dependent on our ability to understand, utilize, manage and maintain the environment we live in - Geoscience is the science that seeks to achieve these goals. This book is a collection of contributions from world-class scientists, engineers and educators engaged in the fields of geoscience and remote sensing.

InTech Europe
University Campus STeP Ri
Slavka Krautzeka 83/A
51000 Rijeka, Croatia
Phone: +385 (51) 770 447
Fax: +385 (51) 686 166
www.intechopen.com

InTech China
Unit 405, Office Block, Hotel Equatorial Shanghai
No.65, Yan An Road (West), Shanghai, 200040, China
中国上海市延安西路65号上海国际贵都大饭店办公楼405单元
Phone: +86-21-62489820
Fax: +86-21-62489821

IntechOpen